Histone deacetylase 4 interacts with 53BP1 to mediate the DNA damage response

Gary D. Kao,[1] W. Gillies McKenna,[1] Matthew G. Guenther,[2] Ruth J. Muschel,[3] Mitchell A. Lazar,[2] and Tim J. Yen[4]

[1]Department of Radiation Oncology, [2]Division of Endocrinology, Diabetes, and Metabolism, Department of Medicine, and
[3]Department of Pathology and Laboratory Medicine, University of Pennsylvania School of Medicine, Philadelphia, PA 19104
[4]Fox Chase Cancer Center, Philadelphia, PA 19111

A number of proteins are recruited to nuclear foci upon exposure to double-strand DNA damage, including 53BP1 and Rad51, but the precise role of these DNA damage–induced foci remain unclear. Here we show in a variety of human cell lines that histone deacetylase (HDAC) 4 is recruited to foci with kinetics similar to, and colocalizes with, 53BP1 after exposure to agents causing double-stranded DNA breaks. HDAC4 foci gradually disappeared in repair-proficient cells but persisted in repair-deficient cell lines or cells irradiated with a lethal dose, suggesting that resolution of HDAC4 foci is linked to repair. Silencing of HDAC4 via RNA interference surprisingly also decreased levels of 53BP1 protein, abrogated the DNA damage–induced G2 delay, and radiosensitized HeLa cells. Our combined results suggest that HDAC4 is a critical component of the DNA damage response pathway that acts through 53BP1 and perhaps contributes in maintaining the G2 cell cycle checkpoint.

Introduction

A number of proteins, including 53BP1 (Schultz et al., 2000; Anderson et al., 2001; Rappold et al., 2001; Xia et al., 2001), Rad51, γH2AX, NBS1/Mre11/Rad50 complex (Maser et al., 1997; Paull et al., 2000), and BRCA1 (Scully et al., 1997; Zhong et al., 1999) have been observed to accumulate at multiple foci in the nucleus in response to DNA damage. 53BP1 was first identified in a yeast two-hybrid screen as one of two proteins that interacted with the trans-activation domain of p53. Recently it was shown that 53BP1 participates in the phosphorylation of p53 and Chk2 and in the maintenance of S and G2 cell cycle checkpoints after DNA damage (DiTullio et al., 2002; Fernandez-Capetillo et al., 2002; Wang et al., 2002). 53BP1 foci are detectable within minutes after exposure to ionizing radiation, the number of foci increases with increasing, and the foci colocalize with that of γH2AX, suggesting an early role in the DNA damage response for 53BP1, as perhaps a marker of unrepaired double-strand breaks. Recent studies of cell lines derived from H2AX knockout mice show that this gene mediates radiation resistance and is essential for various components of the DNA damage response pathway to form foci (Bassing et al., 2002; Celeste et al., 2002). Although these data point to a role of chromatin in the DNA damage response, it remains unclear to what extent these foci represent alterations of the underlying chromatin.

Chromatin undergoes expansion and compaction in the course of many fundamental cellular processes, including gene expression, differentiation, and cell cycle progression. These alterations of the chromatin are largely mediated by histone acetylases and histone deacetylases (HDACs).* HDACs act on key acetylated lysine residues of core histones to induce chromatin compaction, which in turn results in gene silencing and heterochromatin formation (Taunton et al., 1996; Yang et al., 1996; Fischle et al., 1999; Grozinger et al., 1999). HDACs have been categorized into three classes that are based on sequence homology and domain organization. Class I HDACs (HDAC1, HDAC2, HDAC3, and HDAC8) are similar to the yeast deacetylase Rpd3 (Yang et al., 1996; Dangond et al., 1998; Emiliani et al., 1998; Buggy et al., 2000; Hu et al., 2000). Class II HDACs (HDAC4, HDAC5, HDAC6, and HDAC7) possess catalytic domains homologous to that of yeast Hda1 (Rundlett et al., 1996; Fischle et al., 1999; Grozinger et al., 1999; Miska et al., 1999; Verdel and Khochbin, 1999;

*Abbreviations used in this paper: ATM, ataxia telangiectasia mutated; DNA-PK, DNA protein kinase; HDAC, histone deacetylase; IR, irradiation; NBS, Nijmegen breakage syndrome; RNAi, RNA interference; siRNA, short interfering RNA; TSA, trichostatin A.

Wang et al., 1999; Kao et al., 2000). Proteins similar to the yeast NAD1-dependent deacetylase Sir2 (Frye, 2000; Imai et al., 2000; Landry et al., 2000; Smith et al., 2000) compose the third class of HDACs. Class I and II HDACs have been found to function as corepressors recruited for transcriptional repression, whereas the class III HDACs are important for gene silencing at telomeres and HM (mating type) loci in yeast (Sherman et al., 1999).

Although HDACs are most prominently linked with transcriptional repression, there are indications that HDACs may play broader roles in regulating cellular processes that affect survival after exposure to DNA-damaging agents. For example, p53 has been found to be deacetylated and inactivated by human Sir2α in mammalian cells, leading to reduced apoptosis and increased survival after exposure to ionizing radiation or etoposide. Conversely, expression of catalytically inactive Sir2α leads to increased apoptosis and radiosensitization in mammalian cells (Luo et al., 2001; Vaziri et al., 2001). Effects of the class III HDACs may extend beyond effects on p53. In budding yeast, members of the SIR2 family of HDACs appear to be important components of the DNA damage pathway. Whereas SIR2 appears to be static, SIR3 and SIR4 are mobilized to sites of DNA breaks (Gottschling et al., 1990; Tsukamoto et al., 1997; Martin et al., 1999; Moazed, 2001). SIR2, SIR3, and SIR4 are required for the efficient recircularization of linear plasmids by nonhomologous end joining, and mutations in these genes resulted in increased sensitivity to γ-radiation in fission yeast (Boulton and Jackson, 1998; Tsukamoto et al., 1997). A role in the DNA damage response has not yet been described for the class I and II HDACs, but is suggested by the observation that treatment with the class I and II HDAC inhibitor trichostatin A (TSA) leads to significant radiosensitization of human cells (Biade et al., 2001) (the class III Sir2 family deacetylases are resistant to TSA [Bernstein et al., 2000]). The mechanism of how TSA might lead to radiosensitization has likewise been unclear.

To assess for a role for class I and II HDACs in the DNA damage response in human cells, we examined several members for their ability to form foci in response to DNA damage. After exposure to double-strand DNA damage in a variety of human cells, we found that human HDAC4 is recruited to nuclear foci with kinetics similar to 53BP1. We found that HDAC4 and 53BP1 colocalize at foci and could be coimmunoprecipitated. HDAC4 foci formation was seen in a wide variety of cell lines, which included radiosensitive cell lines lacking the gene products of ATM (ataxia telangiectasia mutated), Nibrin, and DNA protein kinase (DNA-PK). HDAC4 foci disappeared after several hours in repair-proficient cells that were exposed to nonlethal doses of radiation. However, HDAC4 foci failed to resolve in radiosensitive cell lines or in normal cells that were exposed to a lethal dose of radiation. Silencing of HDAC4 resulted in decreased 53BP1 protein levels and did not markedly affect cell cycle distribution in unirradiated cells, but markedly abrogated the G2 checkpoint in radiosensitized cells after DNA damage. These results together suggest that HDAC4 is a critical component of the DNA damage response pathway and suggests an additional role for this protein beyond transcriptional silencing.

Results

HDAC4 is recruited to nuclear foci after exposure to double-strand DNA damage

To investigate a potential role of HDACs in the DNA damage response in human cells, we studied the response of HDAC2, 4, and 6 to DNA damage. HeLa cells exposed to γ-irradiation (IR) or etoposide exhibited distinct foci of HDAC4 in their nucleus (Fig. 1, B and D), whereas unirradiated (Fig. 1 A) or UV exposure did not have this effect (Fig. 1 E). In contrast, DNA damage did not induce foci formation by HDAC2 (Fig. 1 I) or HDAC6 (Fig. 1 J) or noticeably alter their intracellular localization. We observed IR-induced HDAC4 foci in both transformed and untransformed cell lines, including the breast cancer cell lines MCF7, PA1, SKBR, and MO59J and K (both of gliomatous origin), the sarcoma cell lines U20S, HT29, and HT1080 (latter two are colon cancer lines), and Wi38 and WSC
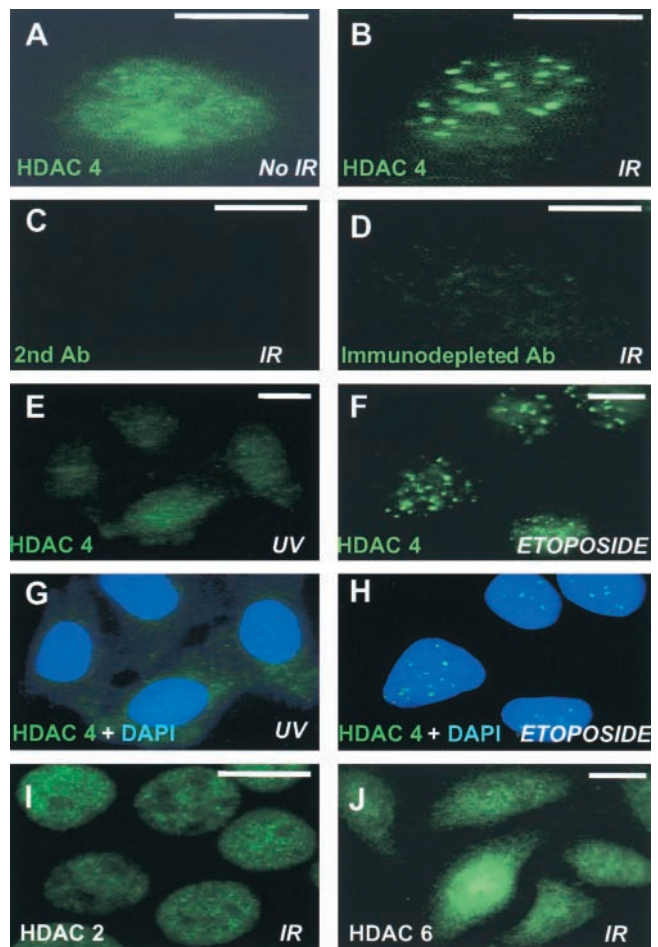

Figure 1. **Recruitment of HDAC4 to nuclear foci after double-strand DNA damage.** HeLa cells that were (A) unirradiated, (B) irradiated with 2 Gy, (C) irradiated and probed with secondary antibody only, (D) irradiated and probed with primary antibody (anti-HDAC4) immunodepleted with the immunizing antigen. (E) HeLa cells exposed to UV (50 J/m²) and (F) 20 μM etoposide were fixed after 1 h and stained with HDAC4 antibodies. (G and H) DAPI stain of cells in E and F, respectively, were merged with HDAC4. Cells irradiated with 2 Gy were stained for (I) HDAC2 and (J) HDAC6. All staining of irradiated cells was performed 1 h after IR. Bar, 5 μm.
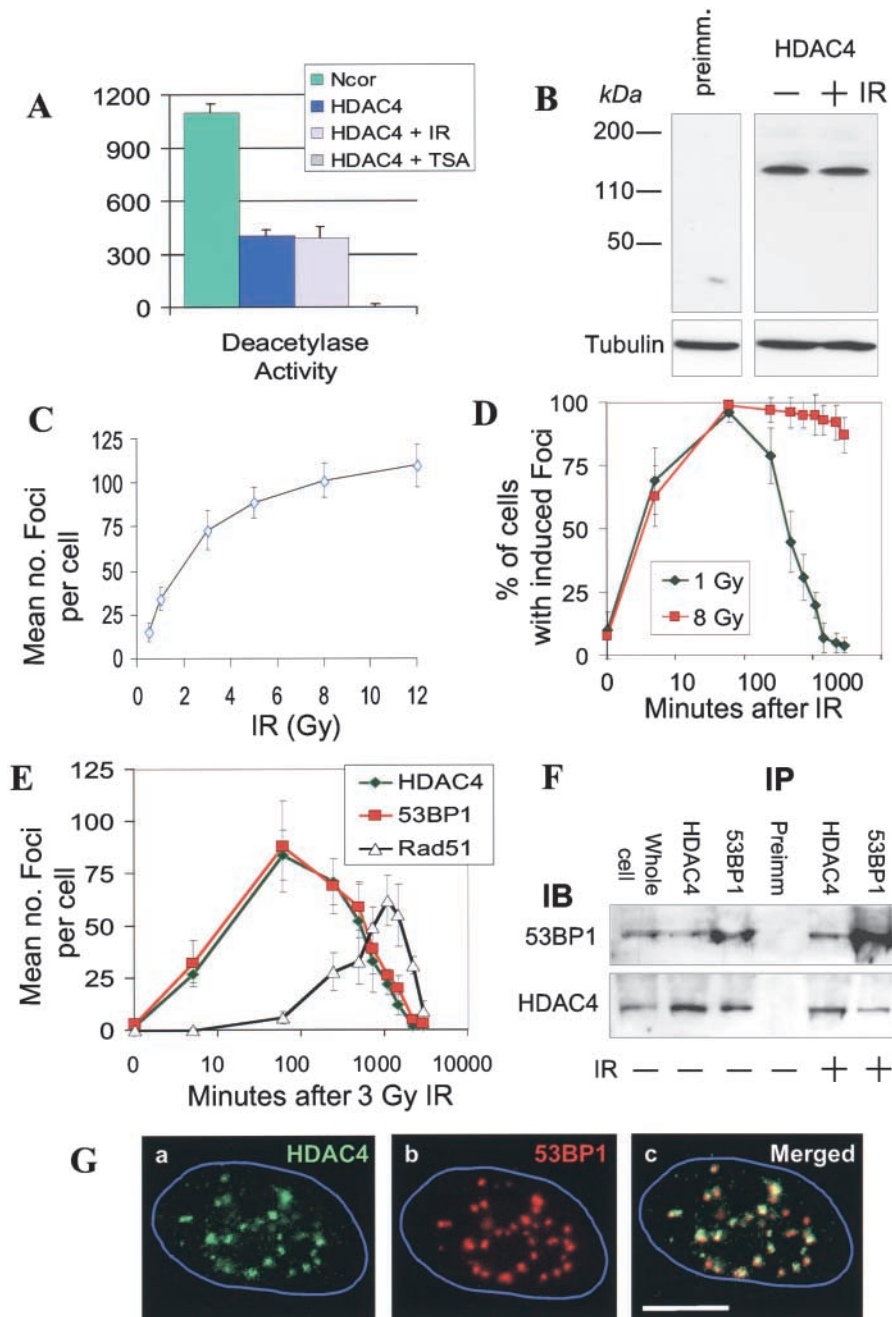
Figure 2. **Dose and time dependency of DNA damage–induced HDAC4 foci.** (A) HDAC4-associated deacetylase activity is not appreciably changed by IR. HDAC4 or Ncor was immunoprecipitated from HeLa lysates and assayed for deacetylase activity. Ncor and HDAC4 treated with TSA serve as positive and negative controls, respectively, for the deacetylase assays. (B) HDAC4 levels do not change after IR. Equal amounts of total protein (25 μg) from HeLa cells were separated via 4–20% gradient SDS-PAGE, transferred to nitrocellulose, and probed with rabbit preimmune serum (left), anti-HDAC4 (right), or anti–α-tubulin antibody (loading control) (bottom). Mock-irradiated (−IR) or irradiated (+IR) cells were harvested 1 h after 3 Gy. (C) HDAC4 foci formation is dependent on the dose of IR. HeLa cells exposed to increasing doses of IR were fixed after 1 h and stained for HDAC4 foci. At least 100 cells were counted for each dose. Error bars represent the SD, and each point represents the average of three experiments. (D) Kinetics of HDAC4 foci formation. HeLa cells irradiated with 1 and 8 Gy were fixed at various times, and the average number of cells showing induced HDAC4 foci was counted. Time is depicted on a log scale. (E) Comparison of the kinetics of foci formation amongst HDAC4, 53BP1, and Rad51. HeLa cells were irradiated (3 Gy), fixed at the indicated times, and separately stained for HDAC4, 53BP1, and Rad51 foci. Error bars represent the SD, and each point represents the average of three experiments. (F) Coimmunoprecipitation of HDAC4 and 53BP1. HeLa cells were lysed in NETN buffer (150 mM NaCl, 1 mM EDTA, 20 mM Tris, pH 8, 0.5% NP-40) and, for each sample, 50 μg of lysate from unirradiated (IR−) or irradiated cells (IR+) was incubated with the indicated antibodies or preimmune serum (IP). The immunoprecipitates were separated on 7.5% SDS-PAGE gels and probed for 53BP1 (top) and HDAC4 (bottom) (IB). Total cell lysate (25 μg, Whole cell) served as a positive control for the immunoblots. (G) Colocalization of HDAC4 foci relative to 53BP1 and Rad51 foci. HeLa cells were irradiated with 3 Gy and 1 h later costained with (a) rabbit anti-HDAC4 and (b) rat anti-53BP1. (c) Images from A and B were merged to reveal that most foci were coincident. The nuclei are outlined in blue. Bar, 5 μm.

(normal human fibroblasts) (unpublished data). Thus, foci formation by HDAC4 in response to DNA damage appears to be a general cellular response that does not appear to be dependent on p53.

The formation of HDAC4 foci after exposure to DNA damage was not accompanied by significant changes in HDAC4 deacetylase activity or protein levels (Fig. 2, A and B). We noted however a dose-dependent increase in the average number of HDAC4 foci per cell (Fig. 2 C). IR resulted in approximately 30 foci per Gy up to 3 Gy, beyond which the increase in the number of foci with increasing dose was difficult to discern. Kinetics of foci formation was

the same between cells exposed to nonlethal (1 Gy) and lethal (8 Gy) doses (Fig. 2 D). HDAC4 foci were evident within 5 min after IR and reached a maximum by 1 h. Interestingly, the number of foci in cells irradiated with 1 Gy progressively decreased to background levels by 24 h after IR. In contrast, the majority (87 ± 7%) of HeLa cells irradiated with 8 Gy retained their HDAC4 foci as long as 48 h after IR. Foci were evident beyond 48 h when there was a high level of cell death (unpublished data). The persistence of HDAC4 foci therefore appears to correlate with lethal doses of IR, which presumably result in accumulation of unrepaired DNA.

HDAC4 interacts with 53BP1

DNA damage induces 53BP1 to form foci within minutes after DNA damage, suggesting that they participate in the early steps of the DNA damage response pathway. In contrast, Rad50 and Rad51 foci appear hours after DNA damage (Paull et al., 2000). We found that HDAC4 formed foci with kinetics very similar to 53BP1. The average number of foci containing either 53BP1 or HDAC4 reached maximal levels by 1 h after 3 Gy and then progressively decreased to near baseline by 36 h (Fig. 2 E). The similarity in the kinetics of HDAC4 and 53BP1 foci formation motivated us to look further for interactions between HDAC4 and 53BP1. Immunoprecipitation experiments showed that HDAC4 and 53BP1 formed a complex in HeLa cells, but the formation of this complex was unaffected by DNA damage (Fig. 2 F). However, immunocytochemical data clearly showed that HDAC4 and 53BP1 colocalized at DNA damage–induced foci (Fig. 2 G). At later times after radiation when Rad51 foci began to accumulate, the numbers of HDAC4 and 53BP1 foci were reduced. The majority of Rad51 foci did not colocalize with HDAC4, although it may be possible that Rad51 was localized to sites that had previously been occupied by HDAC4 (see Figs. S1 and S2, available at http://www.jcb.org/cgi/content/full/jcb.200209065/DC1).

HDAC4 foci induced by IR persist in radiosensitive cells

We next examined in a range of human cell lines the genetic determinants that specified HDAC4 foci formation. We found that HDAC4 foci formation did not depend on DNA damage response genes, i.e., ATM (ataxia telangiectasia mutated), Nibrin, or DNA-PK, as cell lines defective for these genes formed foci with similar kinetics as HeLa cells (Fig. 3). However, the repair-deficient cell lines differed from HeLa (and other repair-proficient) cells in the persistence of HDAC4 foci after exposure to low doses of IR. For example, HDAC4 foci readily formed 1 h after radiation in the ATM-deficient FT169 cell line, as well as in its isogenic derivatives Y25 (in which ATM is restored by expression of a full-length cDNA) and PEB (expressing empty vector and hence remaining ATM deficient). 24 h after IR, HDAC4 foci were significantly reduced only in the ATM-positive Y25 cells (Fig. 3, A–D). A similar difference in the resolution of HDAC4 foci was observed between DNA-PK–deficient MO59J cells and DNA-PK–positive MO59K cells. Al-

Figure 3. **DNA repair–deficient cell lines are unable to efficiently resolve HDAC4 foci.** Cells deficient for ATM, DNA-PK, and Nibrin were exposed to 1 Gy of IR and fixed and stained for HDAC4 1 and 24 h after IR. The average percentage of each cell line showing IR-induced HDAC4 was determined and the data presented in a histogram. Representative images of the HDAC4 staining pattern in the respective cell lines 24 h after IR are presented in the right panels. (A) 1 h after IR (1 Gy), respectively 95 ± 4.3% and 89 ± 4.0% of ATM-deficient FT169A and ATM-restored Y25 cells showed induced foci, a difference that was statistically insignificant. In contrast, 24 h after IR, respectively 82 ± 3.1% and 33 ± 5.9% of FT169A and Y25 cells showed induced foci (P < 0.001). PEB cells, derived from FT169A cells via stably transfecting with the empty parental vector (and which remain deficient for ATM protein and radiosensitive) continued to show high levels of induced HDAC4 foci after IR. Representative images of (B) FT169A (ATM−), (C) Y25 (ATM+), and (D) PEB (ATM control) cell lines 24 h after IR. (E) 1 h after IR, respectively 93 ± 6.7% and 95 ± 3.4% of DNA-PK–deficient MO69J and DNA-PK–proficient MO59K cells showed induced foci, a difference that was not significant. In contrast, 24 h after IR, respectively 86 ± 10.5% and 40 ± 9.6% of MO59J and MO59K showed induced foci (P < 0.001). Representative images of (F) MO59J (DNAPK−) and (G) MO59K (DNAPK+) cells 24 h after IR. In the MO59K cells with persistent foci, the number of foci per cell was also consistently fewer than in the MO59J cells (average of 11 ± 3.1 vs. 45 ± 3.7 foci, respectively, per MO59K vs. MO59J cell; P < 0.001). (H) Nibrin-deficient cells (NBS−) showed high levels of HDAC4 foci at both 1 (95 ± 5.4% of cells) and 24 h (83 ± 2.6%) after

% of cells showing Induced Foci

1 hour after 1 Gy 24 hour after 1 Gy

IR. In contrast, respectively 89 ± 2.4% and 9 ± 3.1% of HeLa cells (HeLa) showed foci. TSA treatment of HeLa cells (HeLa + TSA) did not prevent foci formation, but inhibited their resolution (93 ± 4.5% and 31 ± 14.5% of HeLa cells pretreated with TSA showed foci at 1 and 24 h after IR). Representative images of (I) Nibrin-deficient (NBS−), (J) HeLa (HeLa), and (K) HeLa cells pretreated with TSA (HeLa + TSA) 24 h after IR. Bar, 5 μm. Data represent the average of three experiments. The nuclei are outlined in blue. Error bars indicate the SD.
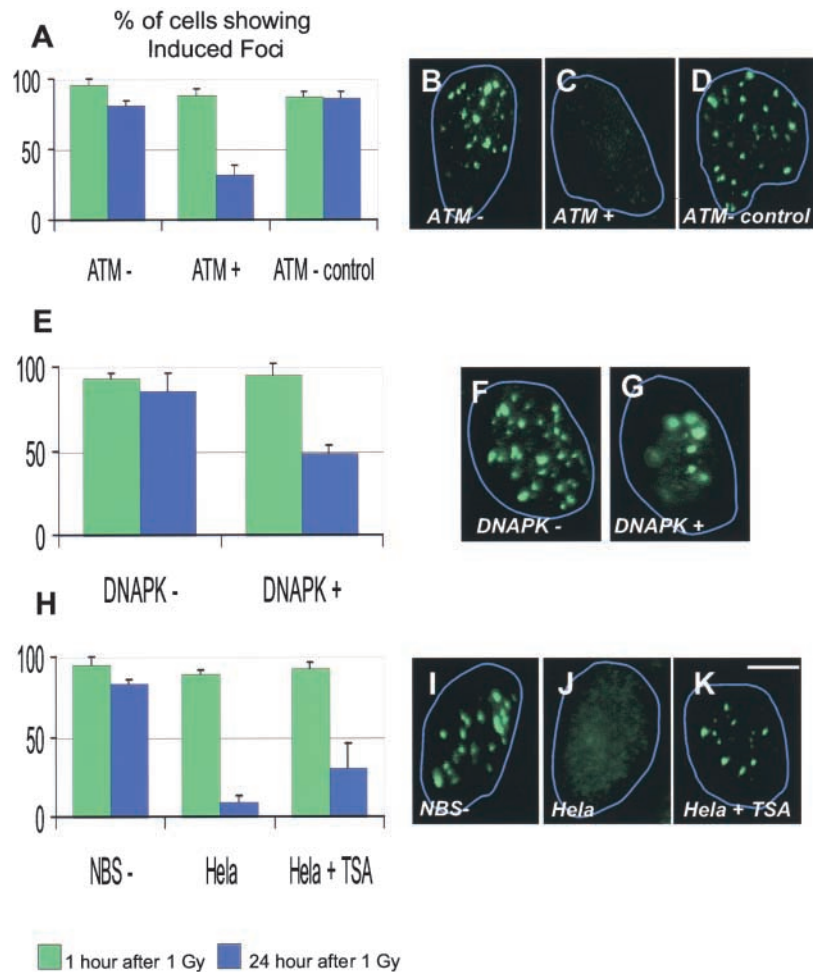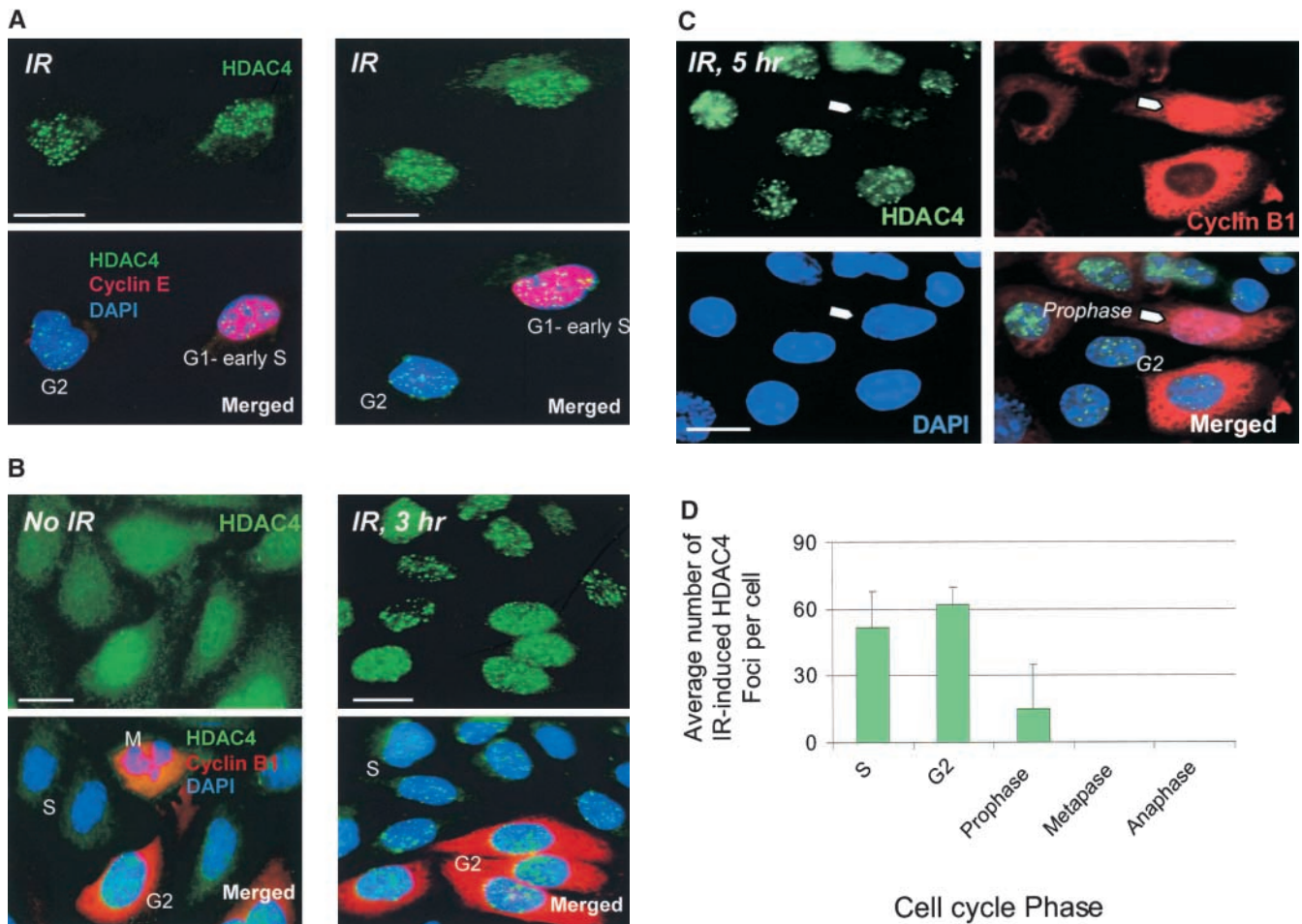
Figure 4. **HDAC4 foci are induced by IR in interphase cells.** (A) Asynchronous HeLa cells were irradiated with 2 Gy IR and 1 h later were fixed and stained for HDAC4, cyclin E, and DAPI. The top panels show HDAC4 staining, and the bottom panels show HDAC4 merged with cyclin E and DAPI. HDAC4 foci are apparent in cells in late G1/early S phase (G1–S) as well as in those not expressing cyclin E and presumably in G2 phase (G2). (B) Cells synchronized and mock irradiated or irradiated (2 Gy) in late S phase were fixed and stained 3 h later for HDAC4, cyclin B1, and DAPI. The top panels show HDAC4 staining, and the bottom panels show HDAC4 merged with cyclin B1 and DAPI. After mock IR (No IR), S-phase cells have not yet expressed cyclin B1 (S), whereas cyclin B1 is cytoplasmic in G2 cells (G2) and coincides with the condensed chromatin in mitotic cells (M) (Kao et al., 1997; Hagting et al., 1999). After IR (IR, 3 h), HDAC4 foci are seen in most cells, including S phase (S) and those that have progressed to and blocked in G2 phase (G2). (C) Synchronized cells were irradiated in late S phase as in B, but fixed 5 h after IR (IR, 5 h). Most cells remain in G2, as indicated by cytoplasmic cyclin B1. However, a few cells have progressed into prophase, as indicated by the entry of cyclin B1 into the nucleus (arrowhead); in these cells, the HDAC4 foci are fewer and less distinct. Bar, 5 μm. (D) Average number of IR-induced HDAC4 foci at each position of the cell cycle. At least 100 cells were counted for each data point, and the experiment was repeated three times with similar results. Error bars represent the SD.

though MO59K cells did not completely resolve their HDAC4 foci, the average number of foci was less than in the MO59J cells (Fig. 3, E–G). We believe that MO59K cells did not efficiently resolve HDAC4 foci because of their inherent radiosensitivity relative to HeLa cells (Wang et al., 1997; unpublished data), which efficiently resolves foci at low doses of IR (Fig. 3 J). Lastly, we examined HDAC4 foci formation in the radiosensitive Nijmegen breakage syndrome (NBS) mutant cell lines and found that they too retained high levels of foci 24 h after IR (Fig. 3, H and I). We found that foci formation by HDAC4 in HeLa cells was unimpeded by TSA. However, the resolution of HDAC4 foci in HeLa cells was partially inhibited by TSA (Fig. 3, H and K).

HDAC4 foci are detected in interphase cells

HDAC4 foci were induced by DNA damage in nearly all cells, suggesting it was not limited to a specific phase of the cell cycle. We sought to confirm this in both asynchronous and synchronized HeLa cells (Fig. 4 A). Using cyclin E expression to distinguish G1–S from G2 cells, we found IR-induced HDAC4 foci in both. Next, we irradiated synchronized cells in S phase and then harvested when cells were beginning to progress into G2 (Fig. 4 B) or mitosis (Fig. 4 C). The average number of foci per cell was not decreased in the G2 cells but, interestingly, was decreased in prophase cells and not evident in mitotic cells (Fig. 4 D). These observations, however, do not permit us to distinguish whether HDAC4 foci form less efficiently in mitotic cells or whether the foci resolve as cells enter mitosis.

Silencing of HDAC4 expression via RNA interference (RNAi) results in decreased 53BP1 protein

To assess further the functions of HDAC4, we silenced its expression by RNA interference (RNAi) (Elbashir et al.,

2001). We found that short interfering RNA (siRNA) directed against two regions of HDAC4 efficiently repressed levels of HDAC4 protein at 48 h after transfection. A control siRNA that was unrelated to HDAC4 had no effect (Fig. 5 A). We conducted a time course experiment to determine the optimal time when HDAC4 expression was at its lowest after siRNA treatment. Considerable amounts of HDAC4 protein were detectable 12 h after transfection, but the level of protein progressively decreased such that very little HDAC4 protein was detectable by 36 h, indicating that
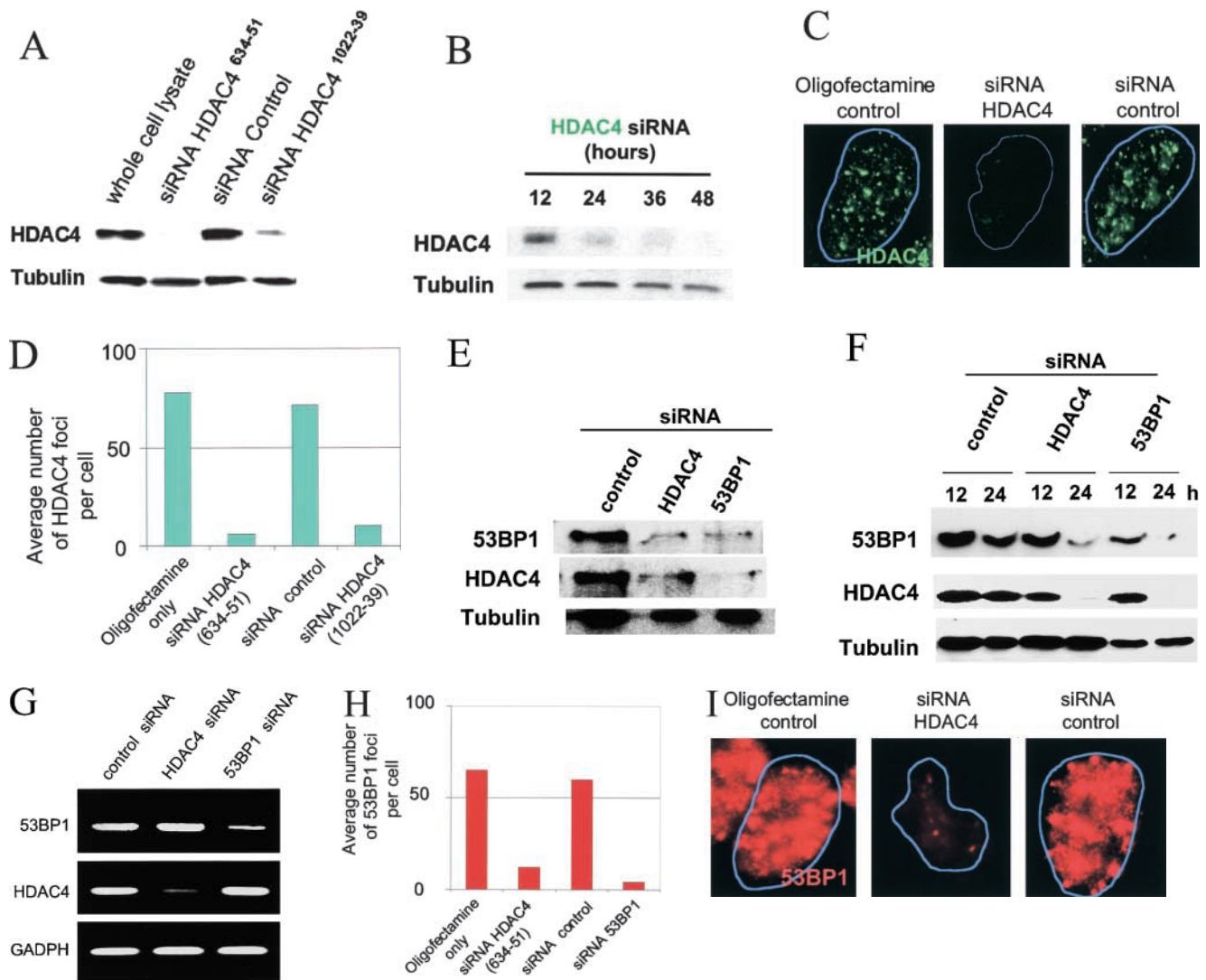

Figure 5. **RNAi efficiently silences HDAC4 and 53BP1 protein expression.** (A) HeLa cells were transfected with siRNA targeting two different sequences in HDAC4 or control siRNA, harvested 36 h later, and immunoblotted for HDAC4 and α-tubulin (loading control). Whole cell lysates from untransfected cells serve as a positive control. (B) Time course of HDAC4 siRNA–mediated silencing of protein expression. Parallel plates of HeLa cells were treated with HDAC4 siRNA and harvested at the times indicated. All lysates were separated on 7.5% SDS-PAGE and immunoblotted for HDAC4 or α-tubulin, indicating maximal silencing of the targeted HDAC4 protein by 36 h. (C and D) HDAC4 siRNA diminishes foci formation after IR. HeLa cells were treated with oligofectamine only, control siRNA, or HDAC4 siRNA and irradiated 36 h later with 2 Gy. 1 h after IR, the cells were fixed and immunofluorescence for HDAC4 was performed. Representative cells are shown in C. The number of HDAC4 foci found in each cell was counted. At least 300 cells were counted for each treatment group. (D) The average number of HDAC4 foci per cell after IR for each treatment group is displayed in the histograms. (E) HDAC4 and 53BP1 siRNA silence expression of their targeted protein, as well as each other. HeLa cells were transfected with HDAC4 or 53BP1 siRNA and harvested 48 h later. Lysates were separated on SDS-PAGE and immunoblotted for 53BP1, HDAC4, and α-tubulin. (F) siRNA-mediated silencing of 53BP1 and HDAC4 protein expression is achieved by 24 h after treatment. Parallel plates of HeLa cells were transfected with 53BP1 siRNA and harvested at the indicated times after transfection. Cell lysates were separated by 7.5% SDS-PAGE and immunoblotted with anti-53BP1, HDAC4, and α-tubulin antibodies. (G) HDAC4 and 53BP1 siRNA reduce only their target mRNA. RT-PCR was performed on total mRNA extracted from HeLa cells 48 h after treatment with control, HDAC4, or 53BP1 siRNA. RT-PCR was performed in parallel under identical conditions using primer pairs targeting 53BP1, HDAC4, or GADPH (as control), and the final product was separated via electrophoresis in ethidium bromide–labeled agarose and photographed under UV illumination. Each RT-PCR reaction yielded a single band as shown. (H and I) HDAC4 siRNA diminishes 53BP1 foci formation after IR. HeLa cells were transfected with oligofectamine control, HDAC4 siRNA, control siRNA, or 53BP1 siRNA and irradiated 36 h later with 2 Gy. 1 h after IR, the cells were fixed, immunofluorescence for 53BP1 was performed, and the average number of foci per cell was determined and displayed in the histograms in H. Representative cells are shown in I.

it is optimal to assess silencing after 24 h (Fig. 5 B). We next examined the effect of the HDAC4 siRNA on foci formation after IR. As expected, HDAC4 foci formation after IR was substantially reduced with both HDAC4 siRNAs, whereas the control siRNA had no effect (Fig. 5, C and D).

We next explored the effect of silencing HDAC4 expression on 53BP1 and were surprised to find that 53BP1 levels were reduced in cells transfected with HDAC4 siRNA (Fig. 5 E). We conducted the converse experiment and found that silencing 53BP1 also led to a reduction of HDAC4. These effects were not seen with a control siRNA. We conducted a time course experiment with both HDAC4 and 53BP1 siRNA and found that levels of either target protein were substantially decreased 24 h after treatment with either siRNA, whereas levels of an unrelated protein (tubulin) were unaffected (Fig. 5 F). To exclude the possibility that the HDAC4 and 53BP1 siRNAs inadvertently precipitated the degradation of 53BP1 and HDAC4 mRNAs, respectively, we assessed the levels of endogenous HDAC4 and 53BP1 mRNA after siRNA treatment. We found that each siRNA reduced only its target mRNA (Fig. 5 G). Thus, the stabilities of HDAC4 and 53BP1 proteins are dependent on each other. Consistent with the observed reduction in protein expression, cells treated with 53BP1 or HDAC4 siRNA showed a dramatic reduction in 53BP1 foci in response to DNA damage (Fig. 5, H and I). Together, these experiments further suggest that HDAC4 interacts in the DNA damage response pathway that involves 53BP1, perhaps as components of the same protein complex.

Silencing of HDAC4 expression via RNAi results in decreased cell viability

We further studied the effects of silencing HDAC4 on cell cycle distribution and cellular viability after DNA damage. Treatment with HDAC4 siRNA did not appear to have a major effect in altering the cell cycle distribution of unirradiated HeLa cells, compared with cells treated with control siRNA (Fig. 6, A and B) or untreated cells (unpublished data). IR of HeLa cells treated with control siRNA resulted in the expected accumulation of cells in G2, characteristic of the IR-induced checkpoint. In contrast, treatment with HDAC4 siRNA markedly decreased the proportion of cells with G2/M DNA content but was accompanied by an increase in cells with DNA content less than 2N (sub-G1) (Fig. 6, A and B). This reduction in G2/M cells was not due to an S-phase delay because HDAC4 siRNA did not affect normal S-phase progression, as determined by FACS® analysis and BrdU incorporation (unpublished data). Flow cytometry based on DNA content alone does not distinguish between cells in G2 and mitosis. We therefore performed immunofluorescence on irradiated cells that were transfected with control and HDAC4 siRNA. Control cells were blocked in G2 after IR, as determined by high cyclin B1 levels in the cytoplasm, CENP-F distributed uniformly in the nucleus, and uncondensed chromatin (Fig. 6, C and D), as described previously (Liao et al., 1995; Kao et al., 2001). In contrast, few of the HDAC4 siRNA–treated cells appeared to be in G2. Although many of these cells still retained cyclin B1 and CENP-F staining, the cyclin B1 was often not uniformly cytoplasmic, the CENP-F staining of the nuclei was frequently uneven, and many of nuclei were condensed

or fragmented. Many of these condensed cells (>70%), in fact, showed high levels of phosphohistone H3 staining, along with cyclin B1, suggesting progression into mitosis (see Fig. S3, available at http://www.jcb.org/cgi/content/full/jcb.200209065/DC1). These observations together suggest that cells silenced for HDAC4 do not maintain a uniform G2 delay after IR. One notes, however, that as 53BP1 has been established to mediate the damage-induced G2 checkpoint, the abrogation of this checkpoint by silencing HDAC4 may be mediated, at least in part, through decreasing 53BP1 protein (DiTullio et al., 2002; Fernandez-Capetillo et al., 2002; Wang et al., 2002).

To further explore the effects on cellular viability of silencing HDAC4 and 53BP1, we performed clonogenic assays to assess the effect on the survival of HeLa cells after DNA damage. Silencing of HDAC4 and 53BP1 had a dramatic effect on the plating efficiency of the cells (Fig. 6 E), indicating that HDAC4 and 53BP1 are likely key determinants of cell proliferation. However, even after correcting for the reduced plating efficiency of these cells, silencing of HDAC4 and 53BP1 further radiosensitized these cells (Fig. 6 F), with 53BP1 having the larger effect of the two. Together, these results suggest that HDAC4 and 53BP1 are required for cells to maintain in G2 after ionizing radiation; when either protein expression is silenced, cells do not block in G2, but instead rapidly lose viability.

Lastly, we examined whether abrogation of the G2 delay occurs when HDACs other than HDAC4 are silenced. Silencing of HDAC2 and HDAC6 did not interfere with the cell's ability to arrest in G2 in response to DNA damage (Fig. 7, A and B). Only silencing of HDAC4 appreciably diminished the proportion of cells delayed in G2 after IR.

Discussion

Our studies have revealed a new role for a HDAC in the DNA damage response pathway. In response to double-stranded DNA breaks, HDAC4, but not HDAC2 or 6, rapidly formed foci that are coincident with the DNA damage response protein 53BP1. Foci formation by HDAC4 occurred throughout interphase and was observed in a wide panel of tumor and normal cell lines. HDAC4 foci formation did not depend on DNA damage response genes ATM, DNA-PK, or NBS, but their resolution was greatly delayed or blocked in these mutant cell lines. This is similar to the finding that ATM is not required for foci formation by 53BP1. When HeLa cells were exposed to a nonlethal dose of IR, where cells are presumably able to repair damaged DNA, HDAC4 foci were efficiently resolved. However, at lethal doses, where cells are presumably unable to effectively repair all of the damaged DNA, the HDAC4 foci persisted. We believe that the efficiency of resolution of HDAC4 foci correlates with cellular radiosensitivity. DNA-PK–defective MO59J cells are highly radiosensitive and were much less efficient at resolving their HDAC4 foci than DNA-PK–positive MO59K cells. MO59K cells, more radiosensitive than HeLa cells, were in turn less efficient at resolving foci than HeLa cells. The failure to resolve HDAC4 foci may reflect the radiosensitizing properties of TSA. These observations together suggest that HDAC4 foci formation is a general cellular response to DNA damage, and
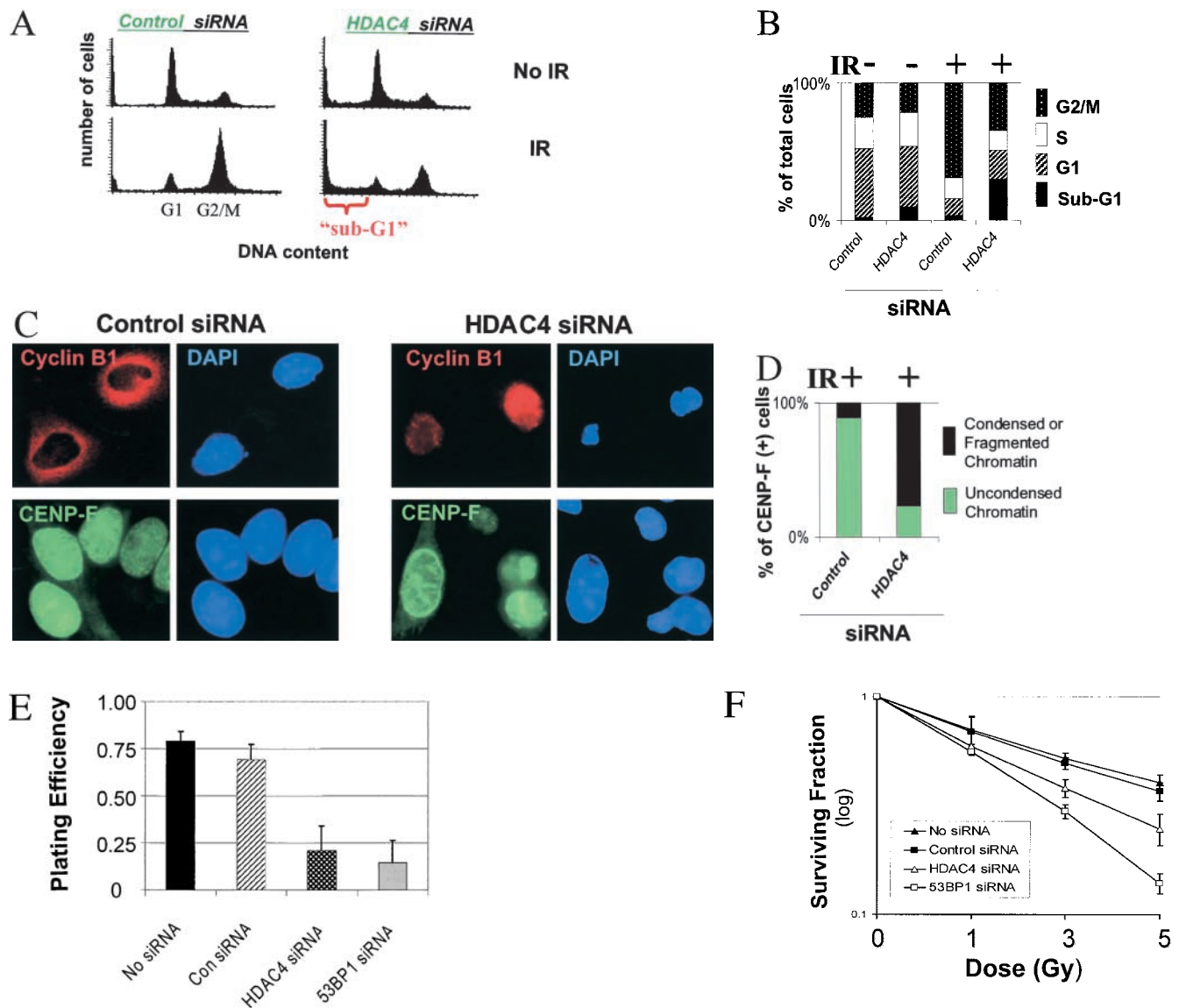
Figure 6. **Silencing of HDAC4 expression abrogates the DNA damage–induced G2 checkpoint and decreases cell viability.** HeLa cells were transfected with control or HDAC4 siRNA, followed 36 h later by mock (No IR) or 5-Gy IR (IR). 8 h after IR, parallel plates of cells were harvested, and cell cycle distribution was analyzed via flow cytometry (A and B) or immunofluorescence (C and D). (A) Silencing of HDAC4 does not have a large effect on unirradiated cells, but it reduced the proportion of irradiated cells with G2/M DNA content. Cells with DNA content less than G1 cells (sub-G1) likely represent apoptotic cells/cell debris, and is especially apparent in cells silenced for HDAC4 and irradiated. (B) Histograms showing cell cycle distribution data from A, indicating the percentage of cells in each part of the cell cycle. The experiment was repeated three times with similar results. (C and D) To better distinguish the proportions of the total population of G2 cells, cells were stained for cyclin B1, CENP-F, and DAPI and analyzed via immunofluorescence. G2-phase cells show cytoplasmic cyclin B1 staining, diffuse nuclear CENP-F staining, and uncondensed chromatin (stained with DAPI) (Liao et al., 1995; Kao et al., 2001). (C) For each pair of images, the left panel shows cyclin B1 or CENP-F staining, and the right panel shows the same cells stained with DAPI. Cells treated with control siRNA show cytoplasmic cyclin B1 and nuclear CENP-F staining, indicative of the IR-induced G2 checkpoint. In contrast, few HDAC4 siRNA–treated cells were blocked in G2, but instead showed fragmented and condensed chromatin that retained cyclin B1 and CENP-F staining. (D) Histogram showing the distribution of CENP-F staining cells with uncondensed (G2 blocked) versus condensed or fragmented chromatin after IR of cells treated with control or HDAC4 siRNA. At least 300 cells were counted for each experiment. (E) Histogram showing plating efficiency of untreated controls or cells treated with control, HDAC4, or 53BP1 siRNA. Cells were plated onto fresh dishes with fresh media 48 h after siRNA treatment, and the proportion of surviving cells capable of excluding Trypan blue was determined 12 h later. The experiment was repeated three times with similar results. Error bars indicate the SD. (F) Survival curves indicating the radiosensitivity of control cells or cells treated with control, HDAC4, or 53BP1 siRNA. Cells were prepared as in E and irradiated with the doses indicated, and the proportion of surviving colonies was determined 2 wk later. All values were corrected for the plating efficiency. Error bars indicate the SD.

conversely, impaired resolution of HDAC4 foci may be correlated with radiosensitivity.

These data suggest that HDAC4 foci may facilitate recruitment of, or stabilize, repair factors such as 53BP1,

which in turn may help maintain damage-induced cell cycle checkpoints. The interaction between HDAC4 and 53BP1 is established here by the findings that the two proteins colocalize and coimmunoprecipitate, as well as the unexpected
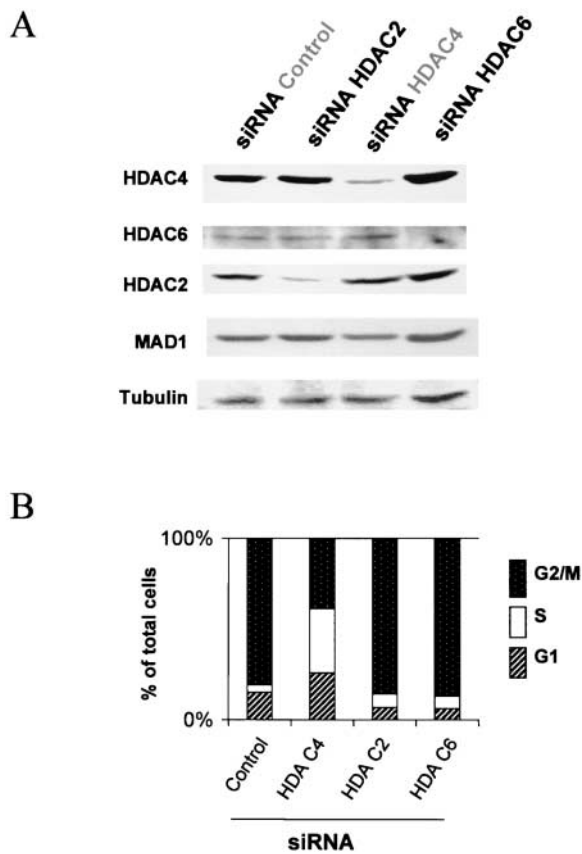
A

B

Figure 7.   **Silencing of HDAC2 and HDAC6 does not abrogate the G2 checkpoint.** Parallel plates of cells were treated with control, HDAC2, HDAC4, or HDAC6 siRNA. 36 h after siRNA treatment, cells were irradiated (5 Gy) and harvested 8 h later for immunoblotting (A) and cell cycle analysis by FACS® (B). (A) Immunoblot of cell lysates from cells treated with siRNA. Cell lysates were separated on 7.5% SDS-PAGE, transferred onto nitrocellulose, and the membranes were probed with anti-HDAC4, HDAC6, HDAC2, Mad1, or α-tubulin antibodies. These show efficient silencing of the target proteins by the HDAC2, 4, and 6 siRNA. Mad1 and α-tubulin are not affected by the specific siRNA treatments and serve as loading controls. (B) Cell cycle distribution of treated cells. Cell cycle analysis shows that the silencing of HDAC4 protein had the most conspicuous effect on abrogation of the G2 checkpoint after IR, relative to silencing of HDAC2 and HDAC6.

findings that siRNA-mediated silencing of HDAC4 leads to reduced levels of 53BP1 protein and vice-versa. Thus, the stability of each protein appears to depend on the stability of the other, or on being associated in a common complex. Our findings that silencing of HDAC4 expression abrogates the damage-induced G2 delay and increases radiosensitivity support the notion that the checkpoint determines the ability of the cell to survive radiation damage. Along with 53BP1, localization of HDAC4 to unrepaired damage may signal the cell to stall at a checkpoint to allow the repair to be completed, while possibly serving as a marker to facilitate repair. These results, therefore, may be consistent with the model proposed by Fernandez-Capetillo et al. (2002) in which 53BP1 and other factors capable of signal transduction may accumulate into a chromatin microenvironment within megabases of an actual DNA double-strand break. This localized concentration of protein complexes may then generate the amplification of signal sufficient to invoke the G2 checkpoint.

These findings do not exclude roles for HDAC4 in mediating other cellular functions. HDAC4 is an established component of complexes mediating transcriptional repression (Guenther et al., 2001; Fischle et al., 2002). Although transcription is globally decreased during mitosis (Spencer et al., 2000; Pflumm, 2002), it appears unlikely that the role of HDAC4 in the DNA damage response is restricted to transcriptional repression. Radiation, at the doses used in this study, does not globally repress transcription (Maity et al., 1995), and drugs that globally inhibit transcription, such as α-amanitin, do not reverse the effects of silencing HDAC4 (unpublished data). The radiation dose dependency of the number of HDAC4 and 53BP1 foci does not exclude, but does reduce, the likelihood that foci are mere storage sites for these proteins.

The recruitment of HDACs to sites of DNA damage may be at least partially evolutionarily conserved. Members of the SIR2 family of HDACs have been implicated in the DNA response in budding yeast, contributing either directly or indirectly to the repair of double-strand breaks (Astrom et al., 1999; Bennett et al., 2001). Whereas SIR2 has been most prominently implicated in the silencing of chromatin at the mating type loci and at telomeres, SIR3 is recruited to sites of DNA damage to form foci that are visible at the cytological level. It has been proposed that the accumulation of some of these deacetylases may induce a repressed chromatin state to facilitate repair or protect unrepaired broken DNA ends (Tsukamoto et al., 1997; Martin et al., 1999). Although HDAC4 does not belong to the same family of deacetylases, we propose that HDAC4 may perform an analogous function in mammalian cells. As a component of protein complexes that mediate transcriptional repression by inducing heterochromatin formation, HDAC4 likely serves a similar role in processing chromatin in the DNA damage response. Recruitment of HDAC4 to foci after DNA damage might reflect its role in silencing the chromatin near the site of damage. The silenced chromatin would prevent processes such as DNA replication and transcription from passing through damaged DNA. In addition, the silenced chromatin might also reduce nonspecific end joining of broken DNA ends or unwanted recombination events.

In linking a HDAC with the DNA damage response to agents inducing double-strand breaks, the results presented here may also have clinical implications for treating patients with cancer. Inhibitors of HDAC inhibitors have entered clinical trials with reports of efficacy in certain tumors (Piekarz et al., 2001; Sandor et al., 2002). These protocols have largely entailed administering the HDAC inhibitor as a single agent. With further development and confirmation, the observations reported here suggest that it may be fruitful to pursue strategies to block HDAC function in combination with standard treatments, such as radiation and chemotherapy, to maximize the killing of cancer cells.

Materials and methods

Antibodies
Polyclonal antibodies were generated by using full-length human HDAC2, 4, and 6 expressed in bacteria to immunize rabbits. For each antigen, the

antibody was purified from at least two rabbits and confirmed to have equivalent specificity. The serum was affinity purified using protein immobilized on Affigel beads (Bio-Rad Laboratories). Specificity of the antibody was further confirmed by preabsorbing purified antibody with the immunizing antigen (Fig. S4, available at http://www.jcb.org/cgi/content/full/jcb.200209065/DC1). Anti-53BP1 antibody was generated against the corresponding domain in human 53BP1 encoded by the 1.5-kb HindIII–EcoRI fragment of XL53BP1 (the 53BP1 cDNA was a gift from Y. Adachi, University of Edinburgh, Edinburgh, UK). Anti-HDAC4, anti-53BP1, anti-Mad1 (gift from M. Campbell, Yen lab), anti–CENP-F (Yen lab), anti–α tubulin (Sigma-Aldrich), and anti–cyclin B1 (BD Biosciences) were used at 1:1,000 for staining and/or immunoblotting. Anti–cyclin E (HE12, sc-247; Santa Cruz Biotechnology, Inc.) and anti-Rad51 antibody (rabbit polyclonal, catalog no. PC130, Oncogene Research Products; mouse monoclonal, RAD51–14B4, GeneTex) was used at 1:500. The anti–phosphohistone H3 antibody recognizes histone H3 phosphorylated on serine 10 (no. 06–570; Upstate Biotechnology) and was used at 1:1,000. Cells were fixed with methanol/acetone 50:50 at the indicated times after IR before staining with the respective antibodies.

Cell lines

All cells were grown in DME medium supplemented with 20% FBS at 37°C with 5% CO_2. The ATM-deficient FT169A (ATM−), ATM-restored YZ5 cells (ATM+, consisting of FT169A transfected with and stably expressing full-length ATM), and ATM-deficient vector-control PEB cells (ATM control, consisting of FT169A cells transfected with the parental vector only) were provided by Y. Shiloh (Tel Aviv University, Ramat Aviv, Israel). Nibrin-deficient human cells were obtained from the American Type Culture Collection. Cells grown on coverslips were irradiated with cesium-137 γ rays from a JL Shepherd and Associates 81–14R panoramic irradiator at a dose rate of 1.35 Gy/min. UV IR was delivered in a single pulse (50 J/m²) using a Stratalinker UV source (Stratagene). Before UV IR, the culture medium was removed, and the medium was replaced immediately after IR. All cells were returned to the incubator for recovery and harvested at the indicated times. Etoposide was used at 20 μg/ml for 20 min. To block cells in mitosis, cells were exposed to 0.04 μg/ml of nocodazole for 15 h.

RNAi

RNAi was performed with siRNA that was commercially synthesized (Dharmacon) and used as described in protocols provided by the manufacturer. Cells were treated with siRNA to a final concentration of 10 μM. siRNA against HDAC6 was applied twice on consecutive days, whereas all other siRNAs were applied once and harvested as described for each experiment. Paired siRNA sequences targeting each protein were as follows: HDAC4, GACGGGCCAGUGGUCACUG and CAGUGACCACUGGC-CCGUC; 53BP1, CACACAGAUUGAGGAUACG and CGUAUCCUCA-AUCUGUGUG; HDAC2, GCCUCAUAGAAUCCGCAUG and CAUGC-GGAUUCUAUGAGGC; HDAC6, CCAGCCAGCGAAGAAGUAG and CUACUUCUUCGCUGCCUGG. Control siRNA consisted of the unannealed single-strand RNA and siRNA targeted against luciferase (both of which did not affect levels of endogenous proteins).

Assays

HDAC assays were performed as previously described (Huang et al., 2000). In brief, [³H]acetylated histones purified from HeLa cells (25,000 cpm/10 μg) were incubated with enzymes at 37°C for 15 min. The reaction was stopped by the addition of concentrated HCl, extracted with 1 ml of ethylacetate, and the amount of radioactivity released into the organic layer was quantitated using a scintillation counter. In experiments in which HDAC4 deacetylase activity was inhibited, HeLa cells were pretreated with 1 μM TSA. For immunoprecipitations, for each sample, 0.1 μg of antibody or 10 μl of preimmune rabbit serum was incubated with cell lysate from 1.0×10^6 cells and incubated in the presence of ethidium bromide (10 μg/ml) to exclude nonspecific protein–DNA associations (Lai and Herr, 1992). Cell preparation, image acquisition and processing, and FACS® analysis were as previously described (Kao et al., 1997, 2001). Endogenous mRNA was isolated using Trizol reagent (GIBCO BRL), as per the manufacturer's instructions, and assessed via RT-PCR. The Titan One Tube RT-PCR System (Roche) was used with the following primers: HDAC4, CAAGAACAAGGAGAAGGGCAAAG and GGACTCTGGTC-AAGGGAACTG; 53BP1, AGGTGGGTGTTCTTTGGCTTCC and TTGGT-GTTGAGGCTTGTGGTGATAC; glyceraldehyde-3-phosphate dehydrogenase, CAACTTTGGTATCGTGGAAGGACTC and AGGGATGATGTT-CTGGAGAGCC (specific details regarding the PCR parameters used are available from the authors).

Plating efficiency was defined as the proportion of cells that remained viable 8 h after trypsinization and replating in fresh media. Cell viability was assessed by trypan exclusion. Clonogenic survival assays were performed as previously described (Biade et al., 2001), except that cells were counted and plated 48 h after treatment with siRNA and colonies of at least 50 cells were counted 14 d after plating. Statistical analyses were performed with SPSS for Windows Release 10 and Microsoft Excel (Office 2000).

Online supplemental material

Additional data (Figs. S1–S4) regarding antibody specificity, Rad51 localization after IR, and phosphorylated histone H3 (Pi-Histone H3) labeling of siRNA-treated cells are available as supplemental material (http://www.jcb.org/cgi/content/full/jcb.200209065/DC1).

References

Anderson, L., C. Henderson, and Y. Adachi. 2001. Phosphorylation and rapid relocalization of 53BP1 to nuclear foci upon DNA damage. *Mol. Cell. Biol.* 21:1719–1729.

Astrom, S.U., S.M. Okamura, and J. Rine. 1999. Yeast cell-type regulation of DNA repair. *Nature.* 397:310–312.

Bassing, C.H., K.F. Chua, J. Sekiguchi, H. Suh, S.R. Whitlow, J.C. Fleming, B.C. Monroe, D.N. Ciccone, C. Yan, K. Vlasakova, et al. 2002. Increased ionizing radiation sensitivity and genomic instability in the absence of histone H2AX. *Proc. Natl. Acad. Sci. USA.* 99:8173–8178.

Bennett, C.B., J.R. Snipe, J.W. Westmoreland, and M.A. Resnick. 2001. SIR functions are required for the toleration of an unrepaired double-strand break in a dispensable yeast chromosome. *Mol. Cell. Biol.* 21:5359–5373.

Bernstein, B.E., J.K. Tong, and S.L. Schreiber. 2000. Genomewide studies of histone deacetylase function in yeast. *Proc. Natl. Acad. Sci. USA.* 97:13708–13713.

Biade, S., C.C. Stobbe, J.T. Boyd, and J.D. Chapman. 2001. Chemical agents that promote chromatin compaction radiosensitize tumour cells. *Int. J. Radiat. Biol.* 77:1033–1042.

Boulton, S.J., and S.P. Jackson. 1998. Components of the Ku-dependent non-homologous end-joining pathway are involved in telomeric length maintenance and telomeric silencing. *EMBO J.* 17(6):1819–1828.

Buggy, J.J., M.L. Sideris, P. Mak, D.D. Lorimer, B. McIntosh, and J.M. Clark. 2000. Cloning and characterization of a novel human histone deacetylase, HDAC8. *Biochem. J.* 350(Pt.1):199–205.

Celeste, A., S. Petersen, P.J. Romanienko, O. Fernandez-Capetillo, H.T. Chen, O.A. Sedelnikova, B. Reina-San-Martin, V. Coppola, E. Meffre, M.J. Difil-ippantonio, et al. 2002. Genomic instability in mice lacking histone H2AX. *Science.* 296:922–927.

Dangond, F., D.A. Hafler, J.K. Tong, J. Randall, R. Kojima, N. Utku, and S.R. Gullans. 1998. Differential display cloning of a novel human histone deacetylase (HDAC3) cDNA from PHA-activated immune cells. *Biochem. Biophys. Res. Commun.* 242:648–652.

DiTullio, R.A., T.A. Mochan, M. Venere, J. Bartkova, M. Sehested, J. Bartek, and T.D. Halazonetis. 2002. 53BP1 functions in an ATM-dependent checkpoint pathway that is constitutively activated in human cancer. *Nat. Cell Biol.* 4:998–1002.

Elbashir, S.M., J. Harborth, W. Lendeckel, A. Yalcin, K. Weber, and T. Tuschl. 2001. Duplexes of 21-nucleotide RNAs mediate RNA interference in cultured mammalian cells. *Nature.* 411:494–498.

Emiliani, S., W. Fischle, C. Van Lint, Y. Al-Abed, and E. Verdin. 1998. Characterization of a human RPD3 ortholog HDAC3. *Proc. Natl. Acad. Sci. USA.* 95:2795–2800.

Fernandez-Capetillo, O., H.T. Chen, A. Celeste, I. Ward, P.J. Romanienko, J.C. Morales, K. Naka, Z. Xia, R.D. Camerini-Otero, N. Motoyama, et al. 2002.

DNA damage-induced G(2)-M checkpoint activation by histone H2AX and 53BP1. *Nat. Cell Biol.* 4:993–997.

Fischle, W., S. Emiliani, M.J. Hendzel, T. Nagase, N. Nomura, W. Voelter, and E. Verdin. 1999. A new family of human histone deacetylases related to *Saccharomyces cerevisiae* HDA1p. *J. Biol. Chem.* 274:11713–11720.

Fischle, W., F. Dequiedt, M.J. Hendzel, M.G. Guenther, M.A. Lazar, W. Voelter, and E. Verdin. 2002. Enzymatic activity associated with class II HDACs is dependent on a multiprotein complex containing HDAC3 and SMRT/N-CoR. *Mol. Cell.* 9:45–57.

Frye, R.A. 2000. Phylogenetic classification of prokaryotic and eukaryotic Sir2-like proteins. *Biochem. Biophys. Res. Commun.* 273:793–798.

Gottschling, D.E., O.M. Aparicio, B.L. Billington, and V.A. Zakian. 1990. Position effect at *S. cerevisiae* telomeres: reversible repression of Pol ll transcription. *Cell.* 63:751–762.

Grozinger, C.M., C.A. Hassig, and S.L. Schreiber. 1999. Three proteins define a class of human histone deacetylases related to yeast Hda1p. *Proc. Natl. Acad. Sci. USA.* 96:4868–4873.

Guenther, M.G., O. Barak, and M.A. Lazar. 2001. The SMRT and N-CoR corepressors are activating cofactors for histone deacetylase 3. *Mol. Cell. Biol.* 21:6091–6101.

Hagting, A., M. Jackman, K. Simpson, and J. Pines. 1999. Translocation of cyclin B1 to the nucleus at prophase requires a phosphorylation-dependent nuclear import signal. *Curr. Biol.* 9:680–689.

Hu, E., Z. Chen, T. Fredrickson, Y. Zhu, R. Kirkpatrick, G.F. Zhang, K. Johanson, C.M. Sung, R. Liu, and J. Winkler. 2000. Cloning and characterization of a novel human class I histone deacetylase that functions as a transcription repressor. *J. Biol. Chem.* 275:15254–15264.

Huang, E.Y., J. Zhang, E.A. Miska, M.G. Guenther, T. Kouzarides, and M.A. Lazar. 2000. Nuclear receptor corepressors partner with class II histone deacetylases in a Sin3-independent repression pathway. *Genes Dev.* 14:45–54.

Imai, S., C.M. Armstrong, M. Kaeberlein, and L. Guarente. 2000. Transcriptional silencing and longevity protein Sir2 is an NAD-dependent histone deacetylase. *Nature.* 403:795–800.

Kao, G., W.G. McKenna, A. Maity, K. Blank, and R.J. Muschel. 1997. Cyclin B1 availability is a rate-limiting component of the radiation-induced G2 delay in HeLa cells. *Cancer Res.* 57:753–758.

Kao, G., W.G. McKenna, and T.J. Yen. 2001. Detection of repair activity during the DNA damage-induced G2 delay. *Oncogene.* 20:3486–3496.

Kao, H.Y., M. Downes, P. Ordentlich, and R.M. Evans. 2000. Isolation of a novel histone deacetylase reveals that class I and class II deacetylases promote SMRT-mediated repression. *Genes Dev.* 14:55–66.

Lai, J.S., and W. Herr. 1992. Ethidium bromide provides a simple tool for identifying genuine DNA-independent protein association. *Proc. Natl. Acad. Sci. USA.* 89:6958–6962.

Landry, J., A. Sutton, S.T. Tafrov, R.C. Heller, J. Stebbins, L. Pillus, and R. Sternglanz. 2000. The silencing protein SIR2 and its homologs are NAD-dependent protein deacetylases. *Proc. Natl. Acad. Sci. USA.* 97:5807–5811.

Liao, H., R.J. Winkfein, G. Mack, J.B. Rattner, and T.J. Yen. 1995. CENP-F is a protein of the nuclear matrix that assembles onto kinetochores at late G2 and is rapidly degraded after mitosis. *J. Cell Biol.* 130:507–518.

Luo, J., A.Y. Nikolaev, S. Imai, D. Chen, F. Su, A. Shiloh, L. Guarente, and W. Gu. 2001. Negative control of p53 by Sir2α promotes cell survival under stress. *Cell.* 107:137–148.

Maity, A., W.G. McKenna, and R.J. Muschel. 1995. Evidence for posttranscriptional regulation of cyclin B1 mRNA in the cell cycle and following irradiation in HeLa cells. *EMBO J.* 14:603–609.

Martin, S.G., T. Laroche, N. Suka, M. Grunstein, and S.M. Gasser. 1999. Relocalization of telomeric Ku and SIR proteins in response to DNA strand breaks in yeast. *Cell.* 97:621–633.

Maser, R.S., K.J. Monsen, B.E. Nelms, and J.H. Petrini. 1997. hMre11 and hRad50 nuclear foci are induced during the normal cellular response to DNA double-strand breaks. *Mol. Cell. Biol.* 17:6087–6096.

Miska, E.A., C. Karlsson, E. Langley, S.J. Nielsen, J. Pines, and T. Kouzarides. 1999. HDAC4 deacetylase associates with and represses the MEF2 transcription factor. *EMBO J.* 18:5099–5107.

Moazed, D. 2001. Common themes in mechanisms of gene silencing. *Mol. Cell.* 8:489–498.

Paull, T.T., E.P. Rogakou, V. Yamazaki, C.U. Kirchgessner, M. Gellert, and W.M. Bonner. 2000. A critical role for histone H2AX in recruitment of repair factors to nuclear foci after DNA damage. *Curr. Biol.* 10:886–895.

Pflumm, M.F. 2002. The role of DNA replication in chromosome condensation. *Bioessays.* 24:411–418.

Piekarz, R., R. Robey, V. Sandor, S. Bakke, W.H. Wilson, L. Dahmoush, D.M. Kingma, M.L. Turner, R. Altemus, and S.E. Bates. 2001. Inhibitor of histone deacetylation, depsipeptide (FR901228), in the treatment of peripheral and cutaneous T-cell lymphoma: a case report. *Blood.* 98:2865–2868.

Rappold, I., K. Iwabuchi, T. Date, and J. Chen. 2001. Tumor suppressor p53 binding protein 1 (53BP1) is involved in DNA damage signaling pathways. *J. Cell Biol.* 153:613–620.

Rundlett, S.E., A.A. Carmen, R. Kobayashi, S. Bavykin, B.M. Turner, and M. Grunstein. 1996. HDA1 and RPD3 are members of distinct yeast histone deacetylase complexes that regulate silencing and transcription. *Proc. Natl. Acad. Sci. USA.* 93:14503–14508.

Sandor, V., S. Bakke, R.W. Robey, M.H. Kang, M.V. Blagosklonny, J. Bender, R. Brooks, R.L. Piekarz, E. Tucker, W.D. Figg, et al. 2002. Phase I trial of the histone deacetylase inhibitor, depsipeptide (FR901228., NSC 630176), in patients with refractory neoplasms. *Clin. Cancer Res.* 8:718–728.

Schultz, L.B., N.H. Chehab, A. Malikzay, and T.D. Halazonetis. 2000. p53 binding protein 1 (53BP1) is an early participant in the cellular response to DNA double-strand breaks. *J. Cell Biol.* 151:1381–1390.

Scully, R., J. Chen, R.L. Ochs, K. Keegan, M. Hoekstra, J. Feunteun, and D.M. Livingston. 1997. Dynamic changes of BRCA1 subnuclear location and phosphorylation state are initiated by DNA damage. *Cell.* 90:425–435.

Sherman, J.M., E.M. Stone, L.L Freeman-Cook, C.B. Brachmann, J.D. Boeke, and L. Pillus. 1999. The conserved core of a human SIR2 homologue functions in yeast silencing. *Mol. Biol. Cell.* 10:3045–3059.

Smith, J.S., C.B. Brachmann, I. Celic, M.A. Kenna, S. Muhammad, V.J. Starai, J.L. Avalos, J.C. Escalante-Semerena, C. Grubmeyer, C. Wolberger, and J.D. Boeke. 2000. A phylogenetically conserved NAD+-dependent protein deacetylase activity in the Sir2 protein family. *Proc. Natl. Acad. Sci. USA.* 97:6658–6663.

Spencer, C.A., M.J. Kruhlak, H.L. Jenkins, X. Sun, and D.P. Bazett-Jones. 2000. Mitotic transcription repression in vivo in the absence of nucleosomal chromatin condensation. *J. Cell Biol.* 150:13–26.

Taunton, J., C.A. Hassig, and S. Schreiber. 1996. A mammalian histone deacetylase related to the yeast transcriptional regulator Rpd3p. *Science.* 272:408–411.

Tsukamoto, Y., J. Kato, and H. Ikeda. 1997. Silencing factors participate in DNA repair and recombination in *Saccharomyces cerevisiae*. *Nature.* 388:900–903.

Vaziri, H., S.K. Dessain, E. Ng Eaton, S.I. Imai, R.A. Frye, T.K. Pandita, L. Guarente, and R.A. Weinberg. 2001. hSIR2(SIRT1) functions as an NAD-dependent p53 deacetylase. *Cell.* 107:149–159.

Verdel, A., and S. Khochbin. 1999. Identification of a new family of higher eukaryotic histone deacetylases. Coordinate expression of differentiation-dependent chromatin modifiers. *J. Biol. Chem.* 274:2440–2445.

Wang, A.H., N.R. Bertos, M. Vezmar, N. Pelletier, M. Crosato, H.H. Heng, J. Th'ng, J. Han, and X.J. Yang. 1999. HDAC4, a human histone deacetylase related to yeast HDA1, is a transcriptional corepressor. *Mol. Cell. Biol.* 19:7816–7827.

Wang, B., S. Matsuoka, P.B. Carpenter, and S.J. Elledge. 2002. 53BP1, a mediator of the DNA damage checkpoint. *Science.* 298:1435–1438.

Wang, J., L. Hu, M.J. Allalunis-Turner, R.S. Day III, and D.F. Deen. 1997. Radiation-induced damage in two human glioma cell lines as measured by the nucleoid assay. *Anticancer Res.* 17:4615–4618.

Xia, Z., J.C. Morales, W.G. Dunphy, and P.B. Carpenter. 2001. Negative cell cycle regulation and DNA damage-inducible phosphorylation of the BRCT protein 53BP1. *J. Biol. Chem.* 276(4):2708–2718.

Yang, W.M., C. Inouye, Y. Zeng, D. Bearss, and E. Seto. 1996. Transcriptional repression by YY1 is mediated by interaction with a mammalian homolog of the yeast global regulator RPD3. *Proc. Natl. Acad. Sci. USA.* 93:12845–12850.

Zhong, Q., C.F. Chen, S. Li, Y. Chen, C.C. Wang, J. Xiao, P.L. Chen, Z.D. Sharp, and W.H. Lee. 1999. Association of BRCA1 with the hRad50-hMre11-p95 complex and the DNA damage response. *Science.* 285:747–750.